

# Competition for light in forest population dynamics: from computer simulator to mathematical model

Pierre Magal <sup>1</sup>  
Zhengyang Zhang <sup>1</sup>

1. Univ. Bordeaux, IMB, UMR 5251, F-33076 Bordeaux, France; CNRS, IMB, UMR 5251, F-33400 Talence, France.

*Keywords:* Computer forest simulator, SORTIE model, size structured model, spatial structured model, state dependent delay differential equations.

*Manuscript type:* Article.

## **Abstract**

In this article we build a mathematical model for forest growth and we compare this model  
3 with a computer forest simulator named SORTIE. The main ingredient taken into account in both  
models is the competition for light between trees. The parameters of the mathematical model  
are estimated by using SORTIE model, when the parameter values of SORTIE model correspond  
6 to the ones previously evaluated for the Great Mountain Forest in USA. We construct a size  
structured population dynamics model with one and two species and with spatial structure.

## Introduction

9 In the natural ecosystem, forests play an important role. This has motivated a lot of people to propose computer simulators as well as mathematical models to describe the dynamical properties of forests. Many computer simulators (also sometimes called Individual Based Models (IBMs)) have been proposed and we refer to JABOWA ([3, 2]), FORET [25], SORTIE [19], FORMIND [9] and others. These models consist of stochastic processes describing individual behaviors, such as birth, death, movement, reproduction and so on. Moreover, these models also permit to describe the behavior of the entire plant community. The main advantage is that it provides simulated data which can be used to analyze such a complex system. Of course this is a rough description of the real plant community. However, they do supply powerful experimental tools and describe the forest dynamics reasonably well [13]. We refer to [14, 21] for a general review about forest IBMs.

SORTIE is a forest simulator based on the forest data observed in and around Great Mountain Forest (GMF), a privately owned 2500ha forest located in northwestern Connecticut (41°57'N, 73°15'W), USA in the year 1990-1992. In SORTIE, four submodels (resource, growth, mortality, and recruitment) are included to determine the behaviour of each individual. As is explained in [19], SORTIE includes only the light limitation as the competition for resources, since little evidence of the effects of water or nitrogen on the growth has been found after extra experiments are performed. Tree growth is described by change of tree size, which is denoted here as the diameter at a certain height. Two concepts "diam<sub>10</sub> (Diameter at 10cm Height)" and "DBH (Diameter at Breast Height)" are often used to describe the tree growth and represent the tree size in the analysis of forest dynamics ([19, 22, 18]). Thereinto, the diam<sub>10</sub> can be used almost throughout the whole life of an individual, from seedling to adult, while DBH can only be used for adults in most cases, as it is measured at a higher height. The definition of the breast height (of an adult human being) is different in different regions, for example, 1.4m in the US and 1.3m in Europe and Canada. But it makes little difference to the measuring result in many cases. We

refer to [29, 19, 20, 22, 8, 18] for more details of SORTIE.

In this article we will extend the model proposed by Hal Smith in [26, 27] to describe the  
36 dynamic of a population that is structured in size with intra-specific competition for light. For a  
single species, we will compare such a mathematical model with SORTIE model for two types of  
tree (American beech (FAGR) and eastern hemlock (TSCA)). Moreover, based on the parameters  
39 estimated separately for each kind of tree, we will investigate the inter-specific competition for  
light by assuming that the growth rate is influenced by the competition for light. We will also  
extend our modelling effort by considering the case of two populations distributed in space and  
42 competing for light.

Several mathematical models describing the forest growth were proposed in the literature.  
Zavala et al. [32] studied a stage-structured population model incorporating the light competi-  
45 tion respectively in growth, mortality and recruitment, and gave the conditions for the existence  
of a steady state distribution. Angulo et al. [1] continued with a similar model, but considering  
the light competition only in recruitment, and they extended it to a two-species stand, and gave  
48 the positive stationary distribution for both single-species and two-species model, and the condi-  
tions for the coexistence. Cammarano [4] studied a system of Lotka-Volterra type, incorporating  
also the light competition and discussed the equilibriums and the coexistence conditions. In this  
51 article, based on SORTIE simulated data, we will exclude the competition occurring in the mor-  
tality and recruitment. In other words, we will see that the best fit for SORTIE model is obtained  
by using a model where the competition for light influences only the growth rate of trees. We  
54 also refer to [6, 28, 10, 17] and the references therein for more kinds of models and researches.

The article is organised as follows. In section 2 we will give a mathematical model for sin-  
gle species, and we will conduct numerical simulations to compare with SORTIE. In section 3  
57 a mathematical model for two species is obtained likewise, and we also conduct the compari-  
son with SORTIE. Then in section 4 we extend it to a 2-dimension spatial model, and conduct  
numerical simulations to see the spread of trees in space.

## 60 Single species model

### Mathematical modelling

In this section we consider the following model describing the growth of trees of single species

$$\left\{ \begin{array}{l} \partial_t u(t, s) + \underbrace{f(A(t)) \partial_s u(t, s)}_{\text{growth of adults}} = - \underbrace{\mu(s)}_{\text{mortality}} u(t, s), \text{ for } t > 0, s > s_-, \\ f(A(t)) u(t, s_-) = \underbrace{\beta b(A(t))}_{\text{flux of newborns}}, \text{ for } t > 0, \\ u(0, \cdot) = u_0(\cdot) \in L^1(0, +\infty). \end{array} \right. \quad (0.1)$$

Here  $u(t, s)$  denotes the population density of trees with size  $s$  at time  $t$ , so  $\int_{s_1}^{s_2} u(t, s) ds$  is the  
 63 number of trees with size  $s \in [s_1, s_2]$  at time  $t$ , and  $A(t)$  is the number of adult population at time  $t$ . The size  $s$  is described by a function of  $\text{diam}_{10}$ , which we will see in the appendix.

The function  $\mu(s) > 0$  is the natural mortality. The minimal size of a juvenile is denoted as  $s_-$ . The parameter  $\beta$  is the birth rate in absence of birth limitation, and the term  $\beta b(A(t))$  describes the flux of newborns into the population, where  $b(x) = xe^{-\xi x}$  is the Ricker's type birth limitation ([23, 24]). The growth function  $f(x)$  takes the form

$$f(x) = \frac{\alpha}{1 + \delta x}, \quad \alpha, \delta > 0, \quad (0.2)$$

which is decreasing, thus taking care of the fact that the more large trees there are, the slower the growth rate of small trees is. So this shows the type of competition for light between adults and juveniles. The function  $u_0(\cdot)$  represents the initial distribution of the species. Normally we want the number of the total population to be finite at each time, hence we have

$$\int_0^{+\infty} u(t, s) ds < +\infty, \quad \forall t \geq 0.$$

So the natural state space for this model is  $L^1$ .

66 We will derive the following equations for adults and juveniles under some assumptions:

$$\left\{ \begin{array}{l} \frac{dA(t)}{dt} = f(A(t))j(t, s^*) - \mu_A A(t), \text{ for } t > 0, \\ \partial_t j(t, s) + f(A(t))\partial_s j(t, s) = -\mu_J j(t, s), \text{ for } s \in [s_-, s^*), t > 0, \\ f(A(t))j(t, s_-) = \beta b(A(t)), \text{ for } t > 0, \\ A(0) = A_0 \geq 0, \\ j(0, s) = j_0(s) \geq 0, \text{ for } s \in [s_-, s^*), \end{array} \right. \quad (0.3)$$

where  $j(t, s)$  represents the population density of juveniles with size  $s \in [s_-, s^*)$  at time  $t$ , and the positive constant  $s^*$  satisfying  $s^* > s_-$  denotes the maximal size of a juvenile (or the minimal size of an adult). Hence the total number of juveniles at time  $t$  is

$$J(t) = \int_{s_-}^{s^*} j(t, s) ds = \int_{s_-}^{s^*} u(t, s) ds.$$

And we can assume as follows the adult population number

$$A(t) = \int_{s^*}^{+\infty} u(t, s) ds. \quad (0.4)$$

By integrating along the characteristic line of the second equation (of juvenile) in (0.3), the first equation (of adult) in (0.3) can be rewritten as the following state dependent Functional Differential Equation (FDE)

$$\left\{ \begin{array}{l} \frac{dA(t)}{dt} = e^{-\mu_J \tau(t)} \frac{f(A(t))}{f(A(t - \tau(t)))} \beta b(A(t - \tau(t))) - \mu_A A(t), \\ \int_{t-\tau(t)}^t f(A(\sigma)) d\sigma = s^* - s_- \end{array} \right. \quad (0.5)$$

when  $t > t^*$ , where  $t^*$  is defined as

$$\int_0^{t^*} f(A(\sigma)) d\sigma = s^* - s_-.$$

Differentiation of the second equation with respect to  $t$  gives the following system

$$\left\{ \begin{array}{l} A'(t) = e^{-\mu_J \tau(t)} \frac{f(A(t))}{f(A(t - \tau(t)))} \beta b(A(t - \tau(t))) - \mu_A A(t), \\ \tau'(t) = 1 - \frac{f(A(t))}{f(A(t - \tau(t)))}. \end{array} \right. \quad (0.6)$$

The initial conditions are

$$A(t) = A_0(t) \geq 0, \forall t \in (-\infty, 0]; \tau(0) = \tau_0 \geq 0, \quad (0.7)$$

where  $A_0(t)$  is continuous and exponentially bounded, namely for some  $\vartheta > 0$

$$\sup_{t \leq 0} e^{\vartheta t} A_0(t) < +\infty.$$

From the second equation of (0.5), as  $f$  is decreasing, the delay  $\tau(t)$  can become large enough, namely we may have infinite delay. For all the derivation here, see Appendix A.

## 69 Numerical simulations of two special cases

We conduct numerical simulations for two special cases of the system (0.5).

**Special case 1 ( $f(x)$  is constant):** Assume that  $f(x)$  is a constant function (so the delay  $\tau(t)$  is also constant by the second equation of (0.5)) and  $b(x) = xe^{-x}$ . Then since the PDE model (0.1) can be transformed (by making a simple change of variable in time) into an age structured model, it is known (see Magal and Ruan [16]) that the system has a Hopf bifurcation around the positive equilibrium when  $\beta$  increases (see in Figure 1).

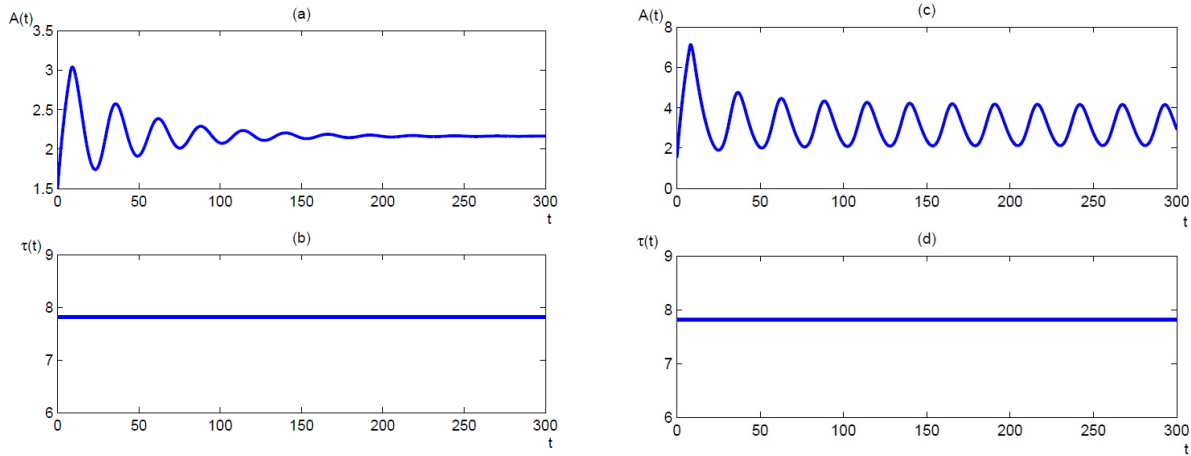


Figure 1: We plot the adult population number  $A(t)$  in figure (a) and (c), and the corresponding delay  $\tau(t)$  in figure (b) and (d). We fix the parameter values  $\mu_I = 0.2$ ,  $\mu_A = 0.1$ ,  $\alpha = 0.5$ ,  $\delta = 0$ ,  $\xi = 1$ ,  $s^* = \ln 50$ ,  $s_- = 0$ , and the initial distribution  $\phi(t) = 1.5, \forall t \in [-100, 0]$ . In (a) and (b) we set  $\beta = 9$ . The solution oscillates and then converges to the positive equilibrium. In (c) and (d) we set  $\beta = 25$ . Changing  $\beta$  from 9 to 25, we observe a Hopf bifurcation.

**Special case 2 ( $b(x) = x$ ):** Assume  $b(x) = x$ , namely the Ricker's type birth function doesn't

appear in system (0.5). It is known that when  $\tau$  is constant in the first equation (which becomes  
78 linear) of system (0.5), this system is either exponentially increasing or exponentially decreasing  
when the time goes to infinity. However, it has been proved by Smith [26] that Hopf bifurcation  
can occur when we take state-dependent delay. This is illustrated in Figure 2.

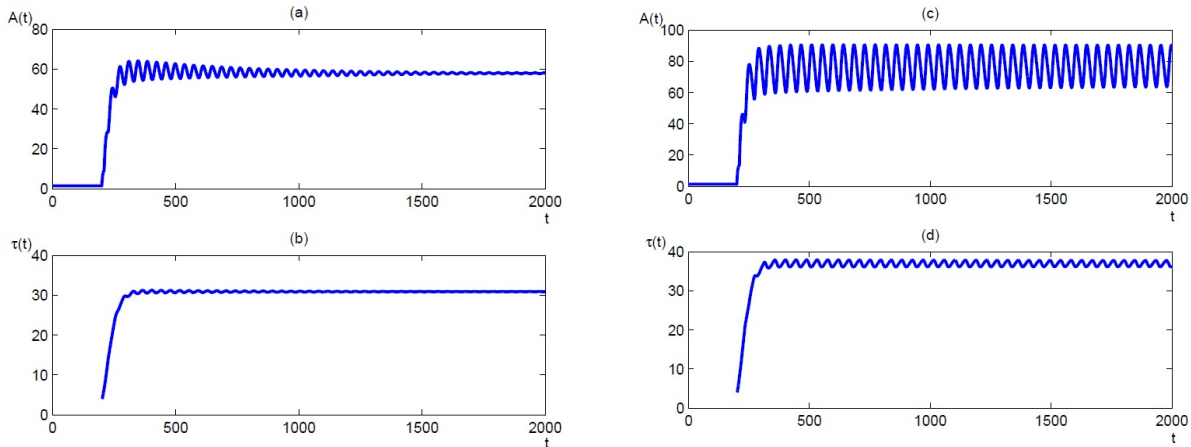


Figure 2: We plot the adult population number  $A(t)$  in figure (a) and (c), and the corresponding delay  $\tau(t)$  in figure (b) and (d). We fix the parameter values  $\mu_J = \mu_A = 0.1$ ,  $\delta = 0.1$ ,  $\xi = 0$  (remember this means that  $b(x) = x$ ), and the initial delay  $\tau_0 = 4$ . The initial distribution is  $\phi(t) = 1.5, \forall t \in [0, 200]$ . In (a) and (b) we set  $\beta = 2.2$ , then we have the damped oscillating solution which converges to the positive equilibrium; In (c) and (d) we set  $\beta = 4$ . Changing  $\beta$  from 2.2 to 4, we observe a Hopf bifurcation.

## 81 Comparison with SORTIE

We run the simulator SORTIE with the parameter values given in [29, 19, 22, 8] and get the  
simulation for the density of adult trees (adults are defined here as trees having a DBH  $\geq 10$ cm).  
84 And as we can see from this simulation, American beech(FAGR) and eastern hemlock(TSCA)  
become the dominant species after a period time. So in this article we will focus on these two  
species in two cases: one single species and two-species.

87 The basic idea of the numerical simulation of (0.5) and comparison is as follows. Before  
starting, we need to get the forest data from SORTIE. Since every run of SORTIE is initiated with  
a random seed, we conduct 50 runs and take the average values as our actual data. Moreover, the



90 data that SORTIE gives are actually the density of the adult population per hectare. As the area of the sample square is  $90000\text{m}^2$  (a square of  $300\text{m} \times 300\text{m}$ ) = 9 hectares, we multiply the data by 9 to obtain the total adult population number. We plot them and the average in MATLAB.

Now we will compare our model (0.5) with the mean value over these 50 runs of SORTIE, and find the best fit. First we need to decide the initial time (for example,  $t = 100$  as the initial time), and we will use the data from SORTIE over the time interval  $[0, 100]$  as the initial condition. Next we discretize the parameters  $\mu_J, \mu_A, \beta, \zeta, \delta, \tau_0$ , and for each set of parameters, we calculate the solution of (0.5) by using the common approximation of the derivative (the numerical scheme will be conducted via the equivalent system (0.6)), and we compare the numerical solutions with the data from SORTIE by using the least square method, to find the set of parameter values with which the numerical result of the model (0.5) and the data have the least difference. Then we use the following formula (see Appendix A)

$$\int_{-\tau_0}^0 \frac{\alpha}{1 + \delta A(\sigma)} d\sigma = s^* - s_-,$$

93 to compute  $\alpha$ , where we use the Simpson's rule to calculate the integral. Now we can keep this set of parameter values, and we have the best fit to SORTIE.

For the first dominant species American beech, we choose the SORTIE data in the time interval  
96  $[0, 200]$  as the initial distribution. We have the best fit in Table 1 and Figure 3.

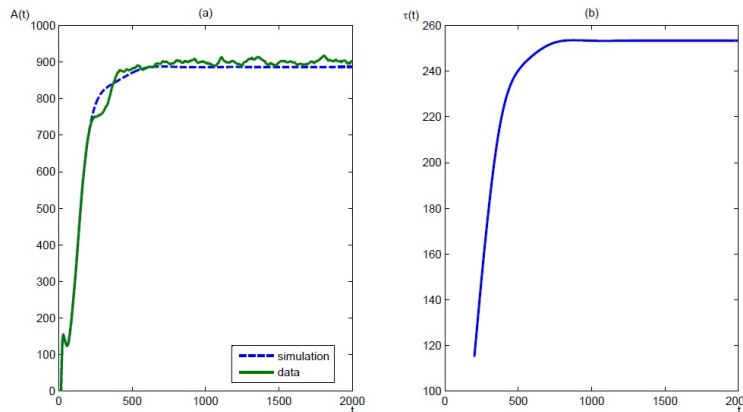


Figure 3: In this figure we show the comparison between SORTIE data and numerical simulation for American beech. The adult population number  $A(t)$  is plotted in (a) and the delay  $\tau(t)$  is shown in (b).

Similarly, for the second dominant species eastern hemlock we choose the SORTIE data in the time interval  $[0,180]$  as the initial distribution. We get the best fit in Table 2 and Figure 4.

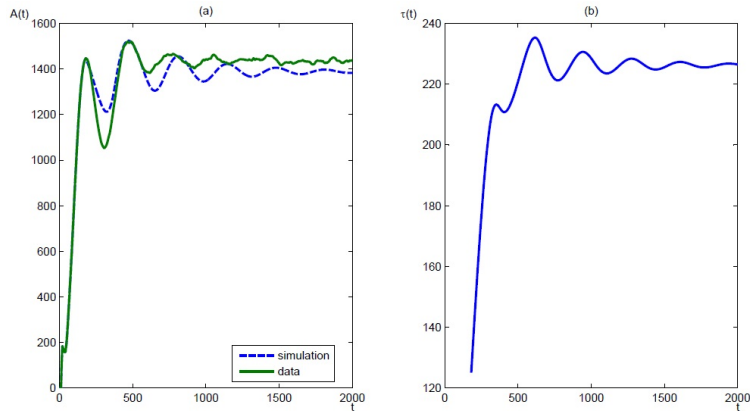


Figure 4: In this figure we show the comparison between SORTIE data and numerical simulation for eastern hemlock. The adult population number  $A(t)$  is plotted in (a) and the delay  $\tau(t)$  is shown in (b). Notice that this species will have an oscillation before it converges to the stable positive equilibrium.

99 Notice that for both species in the single species case, we have  $\zeta_1 = \zeta_2 = 0$  as the best fit, which means that there is no Ricker's type birth limitation here.

## Two-species model

### 102 Mathematical modelling

System (0.1) can be extended to the case of two species. Taking the previous best fit  $\zeta_1 = \zeta_2 = 0$  into account, we obtain the following system

$$\left\{ \begin{array}{l} \partial_t u_1(t, s) + f_1(Z_1(t)) \partial_s u_1(t, s) = -\mu_1(s) u_1(t, s), \text{ for } t > 0, s > s_-, \\ \partial_t u_2(t, s) + f_2(Z_2(t)) \partial_s u_2(t, s) = -\mu_2(s) u_2(t, s), \text{ for } t > 0, s > s_-, \\ f_1(Z_1(t)) u_1(t, s_-) = \beta_1 A_1(t), \text{ for } t > 0, \\ f_2(Z_2(t)) u_2(t, s_-) = \beta_2 A_2(t), \text{ for } t > 0, \\ u_1(0, \cdot) = u_{10}(\cdot) \in L^1(0, +\infty), \\ u_2(0, \cdot) = u_{20}(\cdot) \in L^1(0, +\infty), \end{array} \right. \quad (0.8)$$

where

$$Z_i(t) = \zeta_{i1} A_1(t) + \zeta_{i2} A_2(t), \quad f_i(x) = \frac{\alpha_i}{1 + \delta_i x}, \quad \mu_i(s) = \begin{cases} \mu_{A_i} > 0, & \text{if } s \geq s^*, \\ \mu_{J_i} > 0, & \text{if } s \in [s_-, s^*), \end{cases}$$

and  $\zeta_{ij} \geq 0$  are nonnegative constants,  $\alpha_i, \delta_i > 0$ ,  $i, j = 1, 2$ . Notice that we use the same minimal juvenile size  $s_-$  and minimal adult size  $s^*$  for both species([19]). After a similar derivation, we have the following state-dependent delay differential equations

$$\left\{ \begin{array}{l} A_i'(t) = e^{-\mu_i \tau_i(t)} \frac{f_i(Z_i(t))}{f_i(Z_i(t - \tau_i(t)))} \beta_i A_i(t - \tau_i(t)) - \mu_{A_i} A_i(t), \\ \int_{t - \tau_i(t)}^t f_i(Z_i(t)) d\sigma = s^* - s_-, \end{array} \right. \quad (0.9)$$

$i = 1, 2$ . We give the following expression for the sake of numerical simulation:

$$\left\{ \begin{array}{l} A_i'(t) = e^{-\mu_i \tau_i(t)} \frac{f_i(Z_i(t))}{f_i(Z_i(t - \tau_i(t)))} \beta_i A_i(t - \tau_i(t)) - \mu_{A_i} A_i(t), \\ \tau_i'(t) = 1 - \frac{f_i(Z_i(t))}{f_i(Z_i(t - \tau_i(t)))}. \end{array} \right. \quad (0.10)$$

## 105 Comparison with SORTIE

We use the same method of comparison as before and we use the parameters in Table 1 and Table 2 to simulate the two-species model. We discretize the new parameters  $\zeta_{ij}$  appeared in the competition term, and also by the least square method, we get the best fit for them:  $\zeta_{11} = 1$ ,  $\zeta_{12} = 0.6$ ,  $\zeta_{21} = 1.6$ ,  $\zeta_{22} = 1$ , and the delay  $\tau_{01}$  is increased to 201,  $\tau_{02}$  increased to 208. We list these values in Table 3. The comparison figure is in Figure 5.

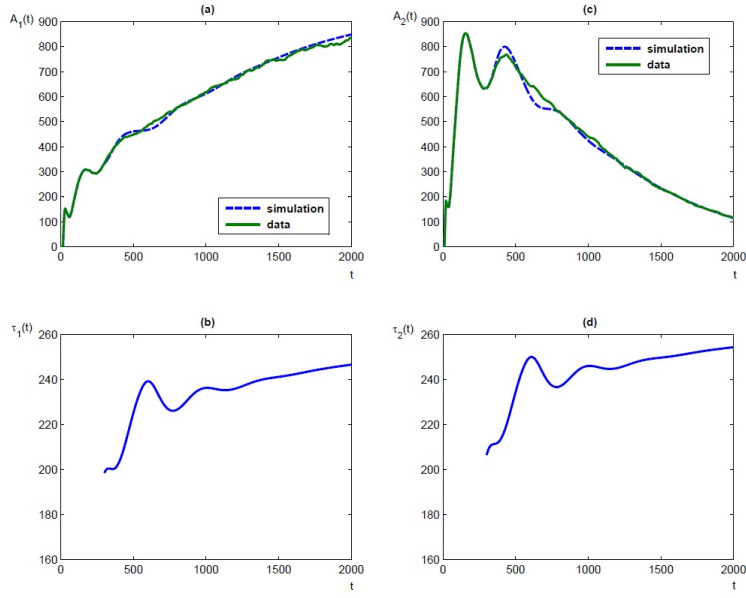


Figure 5: In this figure we plot the comparison between SORTIE data and numerical simulation for two-species model (0.9). The figures (a) and (c) show the adult population number for species 1 American beech and species 2 eastern hemlock respectively. The figures (b) and (d) show the corresponding time delay.

111 By analyzing the existence positive (coexisting) equilibrium (see Appendix B), we can also obtain the coexistence of both American beech and eastern hemlock.

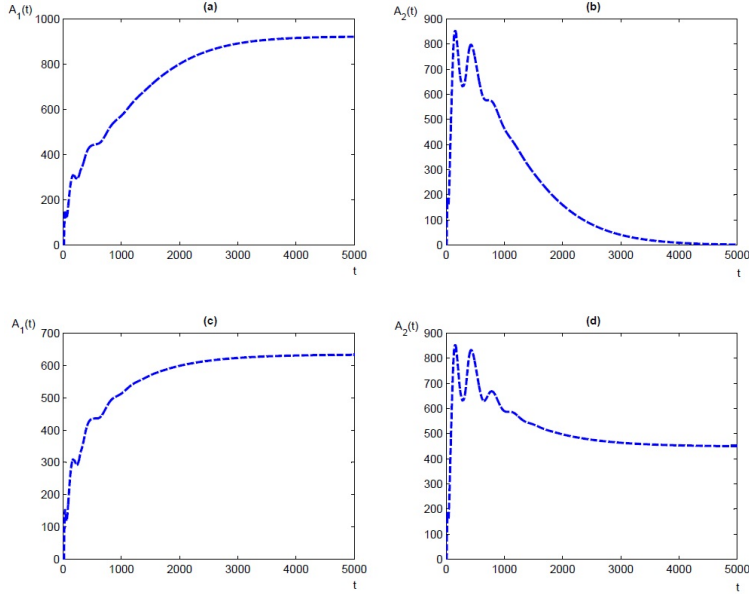


Figure 6: In this figure we demonstrate that we can pass from competitive exclusion (a)(b)(which corresponds to Figure 5) to coexistence (c)(d) by changing one parameter  $\zeta_{21}$ . The other parameters are the same as in Figure 5. When  $\zeta_{21} = 1.6$ , American beech (a) reaches to a positive steady state while eastern hemlock (b) disappears gradually. After we decrease the value of  $\zeta_{21}$  to 1, both American beech (c) and eastern hemlock (d) go to a positive steady state, which means coexistence.

## Two-species spatial model

114

Now we take the spatial position of the individuals into account to see the spread of the adult population. Inspired by Ducrot [7], we can describe the spreading of the seeds around the adult trees by using the following two species model

$$\left\{ \begin{array}{l} \partial_t u_i(t, s, x, y) + f_i(Z_i(t, x, y)) \partial_s u_i(t, s, x, y) = -\mu_i(s) u_i(t, s, x, y), \\ \quad \text{for } t > 0, s > s_-, x \in [0, x_{\max}], y \in [0, y_{\max}], \\ f_i(Z_i(t, x, y)) u_i(t, s_-, x, y) = (I - \varepsilon_i \Delta)^{-1} (\beta_i A_i(t, \cdot, \cdot))(x, y), \\ \quad \text{for } t > 0, x \in [0, x_{\max}], y \in [0, y_{\max}], \\ u_i(t, x, 0) = u_i(t, x, y_{\max}), \text{ for } x \in [0, x_{\max}], \\ u_i(t, 0, y) = u_i(t, x_{\max}, y), \text{ for } y \in [0, y_{\max}], \\ u_i(0, s, x, y) = u_{i0}(s, x, y) \in L^1((0, +\infty) \times [0, x_{\max}] \times [0, y_{\max}]), \end{array} \right. \quad (0.11)$$

where

$$Z_i(t, x, y) = \zeta_{i1} A_1(t, x, y) + \zeta_{i2} A_2(t, x, y), f_i(x) = \frac{\alpha_i}{1 + \delta_i x},$$

$\zeta_{ij} \geq 0$ ,  $\alpha_i, \delta_i > 0$ ,  $i = 1, 2$ , and  $\Delta$  is the Laplacian operator with periodic boundary condition.

Similarly, we assume the adult population number

$$A_i(t, x, y) = \int_{s^*}^{+\infty} u_i(t, s, x, y) ds, i = 1, 2,$$

and by following a similar procedure as before, we get the state-dependent delay differential equation for the adult

$$\left\{ \begin{array}{l} \frac{\partial A_i(t, x, y)}{\partial t} = e^{-\mu_i \tau_i(t, x, y)} \frac{f_i(Z_i(t, x, y))}{f_i(Z_i(t - \tau_i(t, x, y), x, y))} (I - \varepsilon_i \Delta)^{-1} (\beta_i A_i(t - \\ \tau_i(t, x, y), \cdot, \cdot))(x, y) - \mu_{A_i} A_i(t, x, y), \text{ for } t > t^*, \\ \int_{t - \tau_i(t, x, y)}^t f_i(Z_i(\sigma, x, y)) d\sigma = s^* - s_-, \text{ for } t > t^*. \end{array} \right. \quad (0.12)$$

117 We conduct numerical simulations for system (0.12), using the parameters in Table 1-3, and  
 120 setting the diffusion coefficient  $\varepsilon_1 = 0.01$ ,  $\varepsilon_2 = 0.005$ , in order to observe the growth and spread  
 of adult population of the two species. The simulation is conducted in a  $300 * 300$  square of the  
 $x - y$  plane, as in the reference [19]. We set the random initial distribution for the two species by  
 taking a random number at 25 random positions.

Next we plot the solutions of system (0.12) at several specified time in Figure 7. The  $x$ - and  
 123  $y$ -axis describe the spatial coordinates, and the  $z$ -axis is the adult population number. In this

figure we will observe the growth of the two species and the spread in space, and we can also see vividly that the model generates obvious species isolates after some time.

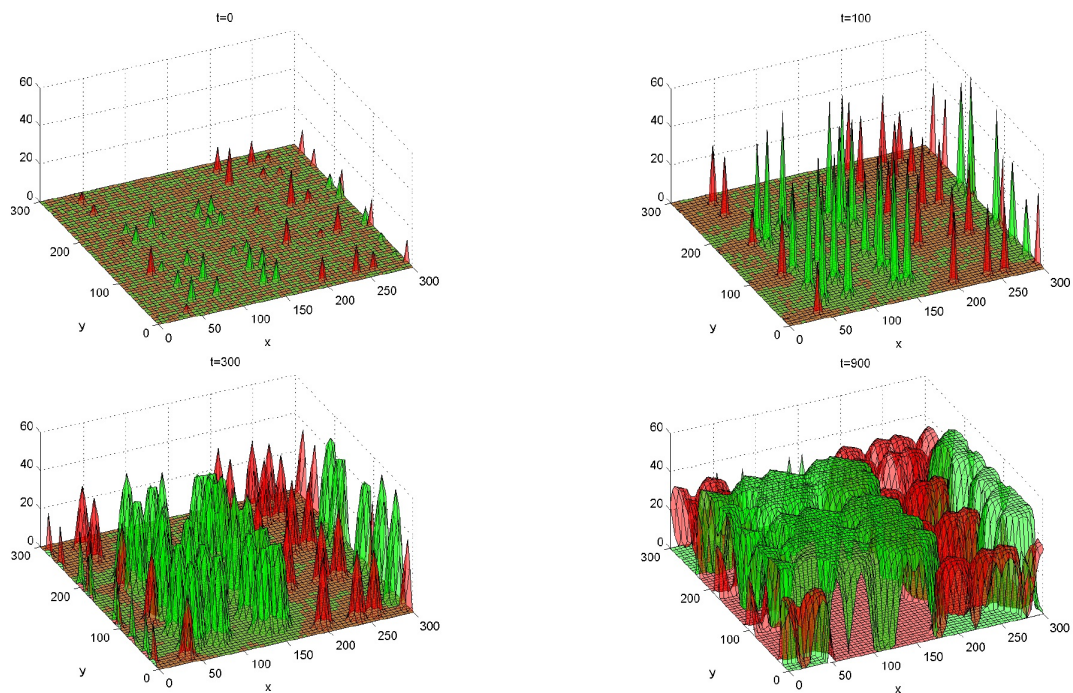


Figure 7: In this figure we show the numerical simulations for the spatial model (0.12), describing the spread of adult population of the two species. The red part represents species 1 American beech, and the green part represents species 2 eastern hemlock.

126

We also conduct the simulation for longer time, and we get the following results in Figure 8.

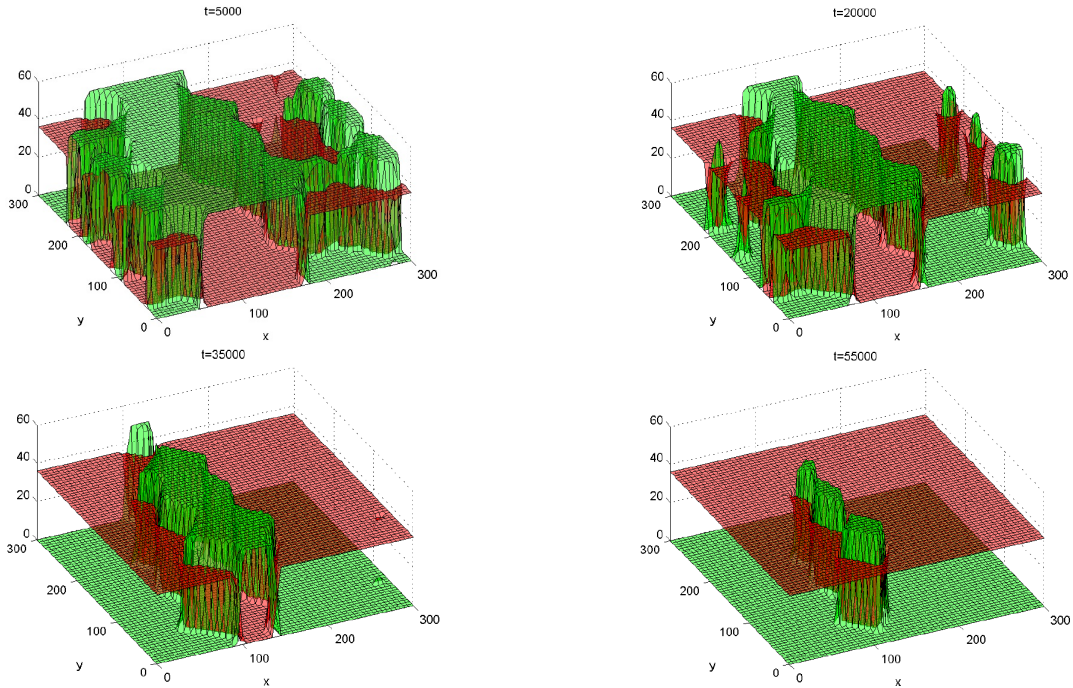


Figure 8: *This figure shows the change of the distribution of adult population of two species in the long run. Notice that eastern hemlock(green) is disappearing and American beech(red) becomes dominant.*

Summarizing all the figures above, we may conclude that eastern hemlock(green) grows and spreads faster than American beech(red) at first, but after long enough time, American beech  
 129 begins to show its competency and gradually becomes the dominant species. This result also coincides with our previous result without considering the space in Figure 5.

Moreover, we plot the total population in the sample square for each species with respect to  
 132 time in Figure 9. And we can see that the total adult population for eastern hemlock increases faster than American beech at first, and then it decreases.



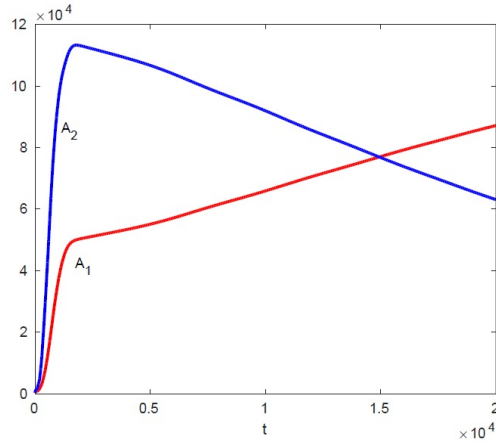


Figure 9: In this figure we show the total population in the  $300m \times 300m$  square for each species in 20000 years.  $A_1$  represents species 1 American beech, and  $A_2$  represents species 2 eastern hemlock.

As in Figure 6, we can also observe the coexistence of both species in the spatial model. In  
 135 Figure 10 we plot the long term distributions after the same change of parameters as in Figure 6.

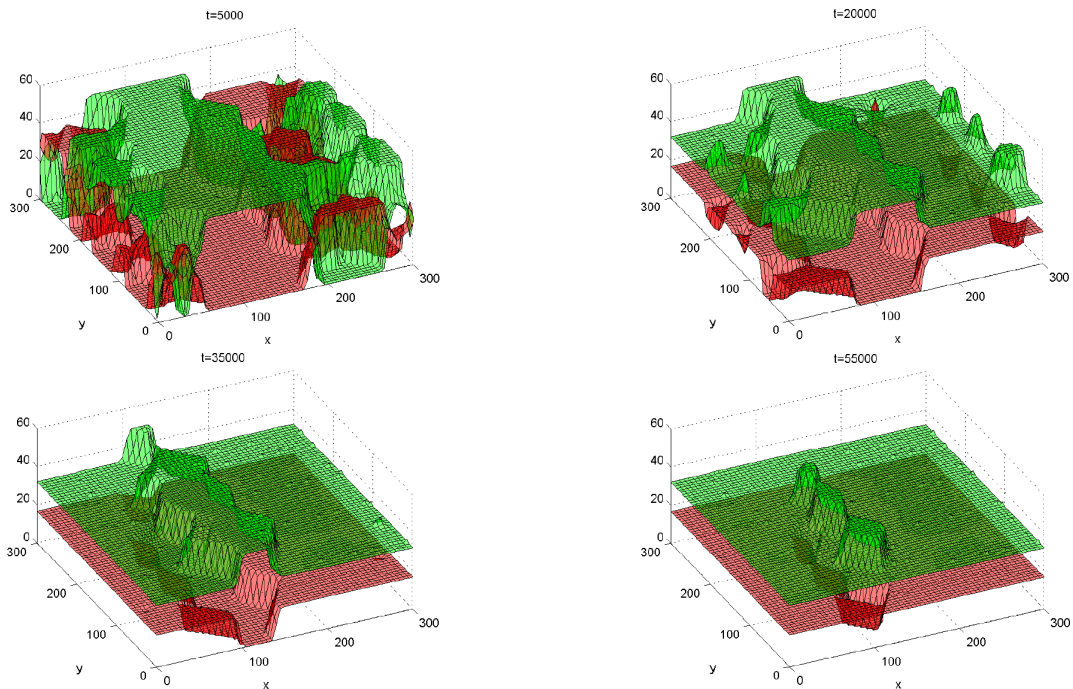


Figure 10: The longterm simulation for the spatial model with a change of the parameter  $\zeta_{21}$  from 1.6 to 1. All the other parameters are the same as in Figure 8. We observe the coexistence of both species.

## Discussion

Studies of forest dynamics have a long history. There have been a large amount of researches  
138 on either the descriptive model for forests reached by observed data, or the pure mathematical  
model with numerical computations, separated from data. Here we first construct a mathematical  
model and compare this model to the computer forest simulator SORTIE. To our best knowledge  
141 there is no similar work in the literature.

We start by fitting the parameters of the model by considering the case of a single species.  
Then for two species, we only fit the parameters corresponding to the competition for light  
144 between the two species of trees. Specifically speaking, we use a classical size-structured model,  
from which we derive a state-dependent delay differential equation, and we use this differential  
equation to fit the forest data from SORTIE. This differential equation is mathematically more  
147 tractable than the submodels in SORTIE.

In order to compare our mathematical model with SORTIE, we conduct numerical simulations  
and we get the best fit to the SORTIE forest data and the corresponding parameter values. One  
150 result we get is that the type of birth function of these two species is not of Ricker's type, as  
we have  $\xi = 0$  in both best fits. We then extend our mathematical model to a two-species case  
with interspecific competition, and similarly we conduct the numerical comparison with SORTIE  
153 forest data, where we also get a very good fit.

Based on this, we go further and propose a model incorporating the spatial position param-  
eter, to describe the density of population, or further, the number of population at every specific  
156 spatial position. We can see vividly the spread and succession in our numerical simulation. By  
using a spatial model, given the initial distribution we will be able to predict specifically the  
population at certain spatial position and time, which is more practical in reality.

159 In our simulation, we reach a result that the population number of eastern hemlock decreases  
to 0 after a long enough time, which conforms to the competitive exclusion principle. However,  
by analyzing the existence of the interior coexistent equilibrium, we are able to establish a range

162 of parameters in which the exclusion principle is no longer true. The coexistence result has also  
 been confirmed by numerical simulations (with and without space). We refer to [32, 4, 10, 1]  
 for more result going into that direction. But there are few results about the coexistence for the  
 165 solution of the structured model. Also it is well known that light is a key influence in many  
 forest systems ([31]), and our model can be used to reproduce the complicated mechanisms  
 included into SORTIE model. But in reality, there are so many influencing factors, such as  
 168 carbon, nitrogen, water, etc.([11, 15, 12, 5, 30]), not only restricted to light. A lot of work is left  
 for future investigation.

## Appendices

### 171 Appendix A Derivation of the state dependent FDE

The single species model (0.1) we consider here is very similar with the one considered by  
 H. Smith in [26]. Nevertheless, our mortality rate  $\mu(s)$  is dependent on the size  $s$ , so we will  
 174 re-derive the state dependent FDE for completeness. Differentiating (0.4) with respect to  $t$ , we  
 have

$$\begin{aligned} \frac{dA(t)}{dt} &= \int_{s^*}^{+\infty} \partial_t u(t, s) ds = -f(A(t)) \int_{s^*}^{+\infty} \partial_s u(t, s) ds - \int_{s^*}^{+\infty} \mu(s) u(t, s) ds \\ &= f(A(t)) u(t, s^*) - \int_{s^*}^{+\infty} \mu(s) u(t, s) ds. \end{aligned} \quad (\text{A.1})$$

Next we deal with the term  $u(t, s^*)$ . The characteristic curves for the first equation in (0.1) are  
 (shown in Figure 11)

$$\frac{ds(t)}{dt} = f(A(t)). \quad (\text{A.2})$$

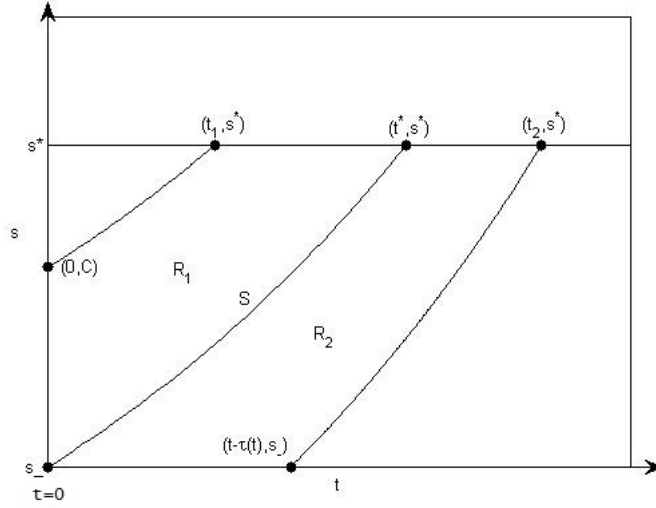


Figure 11: In this figure we present the characteristic curves (A.2).

Then we will have the following representation of  $s$

$$C + \int_0^t f(A(\sigma))d\sigma = s(t). \quad (\text{A.3})$$

Suppose  $t^*$  is the time when juveniles present at time 0 become adults, namely

$$\int_0^{t^*} f(A(\sigma))d\sigma = s^* - s_-. \quad (\text{A.4})$$

We can see that the curve

$$S = \left\{ (t, s) : 0 \leq t \leq t^*, s = s_- + \int_0^t f(A(\sigma))d\sigma \right\}$$

divides the strip  $[0, +\infty) \times [s_-, s^*]$  into two parts  $R_1$  and  $R_2$ . Assuming that  $s - s_- \leq \int_0^t f(A(\sigma))d\sigma$ , then we can find  $T(t, s) \geq 0$  such that

$$\int_{t-T(t,s)}^t f(A(\sigma))d\sigma = s - s_- \quad (\text{A.5})$$

in the region  $R_2$ , so it denotes the time it takes for a juvenile to grow to size  $s$  at time  $t$  from the

177 minimal size  $s_-$ . Replacing  $s$  in  $u(t, s)$  with (A.3), we can compute formally as follows, assuming

that  $u$  is a  $C^1$ -function:

$$\begin{aligned}
& \frac{d}{dt} u \left( t, C + \int_0^t f(A(\sigma)) d\sigma \right) \\
&= \partial_t u \left( t, C + \int_0^t f(A(\sigma)) d\sigma \right) + f(A(t)) \partial_s u \left( t, C + \int_0^t f(A(\sigma)) d\sigma \right) \\
&= -\mu \left( C + \int_0^t f(A(\sigma)) d\sigma \right) u \left( t, C + \int_0^t f(A(\sigma)) d\sigma \right).
\end{aligned}$$

This is a separable ODE with respect to  $t$ . Integration of this equation, and by using the initial distribution and the boundary condition, we obtain the following expression of  $u(t, s)$

$$u(t, s) = \begin{cases} u_0 \left( s - \int_0^t f(A(\sigma)) d\sigma \right) e^{-\int_0^t \mu(s - \int_0^l f(A(\sigma)) d\sigma + \int_0^l f(A(\sigma)) d\sigma) dl}, & \text{if } s \geq s_- + \int_0^t f(A(\sigma)) d\sigma, \\ \frac{\beta b(A(t - T(t, s)))}{f(A(t - T(t, s)))} e^{-\int_{t-T(t, s)}^t \mu(s_- + \int_{t-T(t, s)}^l f(A(\sigma)) d\sigma) dl}, & \text{if } s \leq s_- + \int_0^t f(A(\sigma)) d\sigma. \end{cases} \quad (\text{A.6})$$

Whenever  $s^* - s_- \leq \int_0^t f(A(\sigma)) d\sigma$ , we can specifically define  $\tau(t) := T(t, s^*)$  as the solution of

$$\int_{t-\tau(t)}^t f(A(\sigma)) d\sigma = s^* - s_-. \quad (\text{A.7})$$

Actually the term  $\tau(t) = T(t, s^*)$  represents the time spent by a newborn becoming an adult.

We now assume the mortality function as follows:

$$\mu(s) = \begin{cases} \mu_A > 0, & \text{if } s \geq s^*, \\ \mu_J > 0, & \text{if } s \in [s_-, s^*]. \end{cases}$$

Then when  $s = s^*$ , we have for  $t \in [0, t^*]$ ,

$$u(t, s^*) = u_0 \left( s^* - \int_0^t f(A(\sigma)) d\sigma \right) e^{-\mu_A t},$$

and for  $t > t^*$ ,

$$u(t, s^*) = \frac{\beta b(A(t - \tau(t)))}{f(A(t - \tau(t)))} e^{-\mu_J \tau(t)}.$$

180 Replacing  $u(t, s^*)$  back in (A.1), we get the model (0.5).

By differentiating the second equation of (0.5) in time, we obtain

$$\frac{d}{dt} \int_{t-\tau(t)}^t f(A(\sigma)) d\sigma = 0 \Leftrightarrow f(A(t)) - f(A(t - \tau(t))) (1 - \tau'(t)) = 0.$$

Therefore the state-dependent delay differential equation (0.6) is derived.

**Remark A.1** *Note that the function  $t \rightarrow t - \tau(t)$  is strictly increasing because*

$$\frac{d}{dt}(t - \tau(t)) = \frac{f(A(t))}{f(A(t - \tau(t)))} > 0.$$

We conduct a comparison between the growth function (0.2) and the intrinsic function of the growth submodel in the simulator SORTIE. From the model (0.3), we only care about the growth of juveniles, so first we assume the radius function of a juvenile

$$r(t) = \frac{\text{diam}_{10}(t)}{2}$$

where  $\text{diam}_{10}$  represents the diameter at 10cm height. We use the following change of variable to define the size  $s$  which we are using in the model (0.1)

$$s(t) := \ln \frac{r(t)}{r_-}, \tag{A.8}$$

where  $r_-$  is the minimal radius of the juvenile. We will have

$$s'(t) = \frac{r'(t)}{r(t)} = f(A(t)).$$

Then the approximation of the derivative of  $r(t)$ , which describes the growth of the radius, is

$$\frac{r(t + \Delta t) - r(t)}{\Delta t} = r(t) \cdot \frac{\alpha}{1 + \delta A(t)} = r(t) \cdot \frac{\alpha A(t)^{-1}}{\delta + A(t)^{-1}}. \tag{A.9}$$

Take  $\Delta t = 1$  (one year), then (A.9) shows the increase of the radius in one year.

On the other hand, we have the following formula for growth in SORTIE from [19, 8, 18]:

$$\text{Annual Radius Increase} = \text{Radius} \cdot \frac{G_1 \cdot \text{GLI}}{\frac{G_1}{G_2} + \text{GLI}}, \tag{A.10}$$

183 where  $G_1$  is the asymptotic growth rate at high light and  $G_2$  is the slope at 0 or low light. The  
term GLI (global light index) describes the percentage of light transmitted through tree gaps and  
perceived by trees, thus is a measure for light. Comparing the two formulas (A.9) and (A.10),  
186 we find that they have the same form, and the parameters  $A(t)^{-1}, \alpha, \delta$  correspond to GLI,  $G_1, \frac{G_1}{G_2}$

respectively. So the choice of the growth function (0.2) is reasonable. Plus, this also explains what is size  $s$  in our model (0.1). By this definition of  $s(t)$ , we have the minimal size of juveniles  $s_- = 0$  (as  $r(t) = r_-$ ), and the minimal size of adults  $s_* = \ln \frac{r^*}{r_-}$ , where  $r^*$  is the minimal radius of adults.

## Appendix B Positive equilibrium for two-species model

We compute the positive equilibrium for the system (0.9), which is, we compute the solution for the following equations:

$$\begin{cases} 0 = e^{-\mu_{J_1}\tau_1}\beta_1 A_1 - \mu_{A_1} A_1, \\ \int_{t-\tau_1}^t \frac{\alpha_1}{1 + \delta_1(\zeta_{11}A_1 + \zeta_{12}A_2)} d\sigma = s^* - s_-, \end{cases} \quad (\text{B.1})$$

and

$$\begin{cases} 0 = e^{-\mu_{J_2}\tau_2}\beta_2 A_2 - \mu_{A_2} A_2, \\ \int_{t-\tau_2}^t \frac{\alpha_2}{1 + \delta_2(\zeta_{21}A_1 + \zeta_{22}A_2)} d\sigma = s^* - s_-, \end{cases} \quad (\text{B.2})$$

Obviously,  $A_1 = 0, A_2 = 0$  is a trivial equilibrium for the species, in which case we have

$$\tau_1 = \frac{s^* - s_-}{\alpha_1}, \quad \tau_2 = \frac{s^* - s_-}{\alpha_2}.$$

Moreover, we have two "boundary" equilibrium  $(\bar{A}_1, 0)$  and  $(0, \tilde{A}_2)$ , where

$$\begin{aligned} \bar{A}_1 &= \frac{1}{\delta_1 \zeta_{11}} \left( \frac{\alpha_1}{\mu_{J_1}(s^* - s_-)} \ln \frac{\beta_1}{\mu_{A_1}} - 1 \right), \\ \bar{\tau}_1 &= \frac{1}{\mu_{J_1}} \ln \frac{\beta_1}{\mu_{A_1}}, \quad \bar{\tau}_2 = \frac{(s^* - s_-)(1 + \delta_2 \zeta_{21} \bar{A}_1)}{\alpha_2}, \end{aligned}$$

and

$$\begin{aligned} \tilde{A}_2 &= \frac{1}{\delta_2 \zeta_{22}} \left( \frac{\alpha_2}{\mu_{J_2}(s^* - s_-)} \ln \frac{\beta_2}{\mu_{A_2}} - 1 \right), \\ \tilde{\tau}_1 &= \frac{(s^* - s_-)(1 + \delta_1 \zeta_{12} \tilde{A}_2)}{\alpha_1}, \quad \tilde{\tau}_2 = \frac{1}{\mu_{J_2}} \ln \frac{\beta_2}{\mu_{A_2}}. \end{aligned}$$

Now we turn to the positive equilibrium. As  $A_1, A_2 \neq 0$ , we solve the first equation in (B.1) and (B.2) and get

$$\tau_1 = \frac{1}{\mu_{J_1}} \ln \frac{\beta_1}{\mu_{A_1}}, \quad \tau_2 = \frac{1}{\mu_{J_2}} \ln \frac{\beta_2}{\mu_{A_2}} \quad (\text{B.3})$$

By the second equation of (B.1) and (B.2), we have

$$\begin{cases} \zeta_{11}A_1 + \zeta_{12}A_2 = \frac{1}{\delta_1} \left( \frac{\alpha_1\tau_1}{s^* - s_-} - 1 \right), \\ \zeta_{21}A_1 + \zeta_{22}A_2 = \frac{1}{\delta_2} \left( \frac{\alpha_2\tau_2}{s^* - s_-} - 1 \right) \end{cases} \quad (\text{B.4})$$

We replace  $\tau_1$  and  $\tau_2$  in (B.4) by (B.3), and we get the following linear equations:

$$\begin{cases} \zeta_{11}A_1 + \zeta_{12}A_2 = \Phi_1, \\ \zeta_{21}A_1 + \zeta_{22}A_2 = \Phi_2, \end{cases} \quad (\text{B.5})$$

where

$$\Phi_1 := \frac{1}{\delta_1} \left[ \frac{\alpha_1}{\mu_{J_1}(s^* - s_-)} \ln \frac{\beta_1}{\mu_{A_1}} - 1 \right], \quad \Phi_2 := \frac{1}{\delta_2} \left[ \frac{\alpha_2}{\mu_{J_2}(s^* - s_-)} \ln \frac{\beta_2}{\mu_{A_2}} - 1 \right].$$

First, as we want a positive solution, we need the following conditions:

$$\Phi_1 \geq 0, \quad \Phi_2 \geq 0. \quad (\text{B.6})$$

We solve the equation (B.5) directly without considering its solvability:

$$A_1 = \frac{\zeta_{22}\Phi_1 - \zeta_{12}\Phi_2}{\zeta_{11}\zeta_{22} - \zeta_{12}\zeta_{21}}, \quad A_2 = \frac{\zeta_{11}\Phi_2 - \zeta_{21}\Phi_1}{\zeta_{11}\zeta_{22} - \zeta_{12}\zeta_{21}}. \quad (\text{B.7})$$

In order to have a positive solution, we need the following conditions:

$$\begin{cases} \zeta_{11}\zeta_{22} - \zeta_{12}\zeta_{21} > 0, \\ \zeta_{22}\Phi_1 - \zeta_{12}\Phi_2 > 0, \\ \zeta_{11}\Phi_2 - \zeta_{21}\Phi_1 > 0, \end{cases} \quad \text{or} \quad \begin{cases} \zeta_{11}\zeta_{22} - \zeta_{12}\zeta_{21} < 0, \\ \zeta_{22}\Phi_1 - \zeta_{12}\Phi_2 < 0, \\ \zeta_{11}\Phi_2 - \zeta_{21}\Phi_1 < 0, \end{cases} \quad (\text{B.8})$$

or in another simplified form

$$\frac{\zeta_{12}}{\zeta_{22}} < \frac{\Phi_1}{\Phi_2} < \frac{\zeta_{11}}{\zeta_{21}}, \quad \text{or} \quad \frac{\zeta_{11}}{\zeta_{21}} < \frac{\Phi_1}{\Phi_2} < \frac{\zeta_{12}}{\zeta_{22}}, \quad (\text{B.9})$$

192

So we have

**Lemma B.1** *Under the condition (B.6) and (B.9), the equations (B.1) and (B.2) have a positive equilibrium as in (B.7).*



We check the conditions (B.6) and (B.9) for our previous results in Table 1-3, and we have

$$\Phi_1 = 100.6839 > 0, \quad \Psi_2 = 133.4324 > 0,$$

$$\frac{\zeta_{12}}{\zeta_{22}} = 0.6, \quad \frac{\Phi_1}{\Phi_2} = 0.7546, \quad \frac{\zeta_{11}}{\zeta_{21}} = 0.625,$$

which does not satisfy the condition (B.9), so there is no positive equilibrium in our previous simulation, and eastern hemlock is disappearing. In order to have a positive equilibrium, we reduce the influence of American beech towards eastern hemlock, namely we lower  $\zeta_{21}$  from 1.6 to 1. Then we have

$$\frac{\zeta_{11}}{\zeta_{21}} = 1,$$

195 which satisfies the condition (B.9). And we have the coexistence of both species as is shown in Figure 6 and Figure 10.

## References

- 198 [1] Ó. Angulo, R. B. de la Parra, J. C. López-Marcos, and M. A. Zavala. Stand dynamics and tree coexistence in an analytical structured model: The role of recruitment. Journal of Theoretical Biology, 333:91–101, 2013.
- 201 [2] D. B. Botkin. Forest dynamics: An ecological model. Oxford University Press, 1993.
- [3] D. B. Botkin, J. F. Janak, and J. R. Wallis. Some ecological consequences of a computer model of forest growth. Journal of Ecology, 60:849–872, 1972.
- 204 [4] M. Cammarano. Co-dominance and succession in forest dynamics: The role of interspecific differences in crown transmissivity. Journal of Theoretical Biology, 285:46–57, 2011.
- 207 [5] A. Cheaïb, A. Mollier, S. Thunot, C. Lambrot, S. Pellerin, and D. Loustau. Interactive effects of phosphorus and light availability on early growth of maritime pine seedlings. Annals of Forest Science, 62:575–583, 2005.

- [6] A. M. de Roos and L. Persson. Competition in size-structured populations: mechanisms  
210 inducing cohort formation and population cycles. Theoretical Population Biology, 63:1–16,  
2003.
- [7] A. Ducrot. Travelling waves for a size and space structured model in population dynam-  
213 ics: Point to sustained oscillating solution connections. Journal of Differential Equations,  
250:410–449, 2011.
- [8] R. K. Kobe, S. W. Pacala, J. A. Silander Jr., and C. D. Canham. Juvenile tree survivorship as  
216 a component of shade tolerance. Ecological Applications, 5(2):517–532, 1995.
- [9] P. Köhler and A. Huth. An individual based rain forest model - concepts and simula-  
tion results. In A. Kastner-Maresch, W. Kurth, M. Sonntag, and B. Breckling, editors,  
219 Individual-based structural and functional models in ecology, volume 52 of Bayreuther  
Forum Ökologie, pages 35–51. Bayreuther Institut für terrestrische Ökosystemforschung,  
Bayreuth, 1998.
- 222 [10] T. S. Kohyama and T. Takada. One-sided competition for light promotes coexistence of forest  
trees that share the same adult height. Journal of Ecology, 100:1501–1511, 2012.
- [11] T. E. Kolb, K. C. Steiner, L. H. McCormick, and T. W. Bowersox. Growth response of north-  
225 ern red-oak and yellow-poplar seedlings to light, soil moisture and nutrients in relation to  
ecological strategy. Forest Ecology and Management, 38:65–78, 1990.
- [12] K. Kramer, I. Leinonen, and D. Loustau. The importance of phenology for the evaluation of  
228 impact of climate change on growth of boreal, temperate and mediterranean forests ecosys-  
tems: an overview. International Journal of Biometeorology, 44:67–75, 2000.
- [13] S. A. Levin, B. Grenfell, A. Hastings, and A. S. Perelson. Mathematical and computational  
231 challenges in population biology and ecosystems science. Science, 275:334–343, 1997.

- [14] J. Liu and P. S. Ashton. Individual-based simulation models for forest succession and management. Forest Ecology and Management, 73:157–175, 1995.
- 234 [15] D. Loustau, S. Crepeau, M. G. Guye, M. Sartore, and E. Saur. Growth and water relations of three geographically separate origins of maritime pine (*pinus pinaster*) under saline conditions. Tree Physiology, 15:569–576, 1995.
- 237 [16] P. Magal and S. Ruan. Center manifolds for semilinear equations with non-dense domain and applications to hopf bifurcation in age structured models. In AMS eBook Collections, volume 202 of Memoirs of the American Mathematical Society. American Mathematical Society, Providence, Rhode Island, 2009.
- 240 [17] N. L. E. Obiang, A. Ngomanda, O. Hymas, É. Chézeauxl, and N. Picard. Diagnosing the demographic balance of two light-demanding tree species populations in central africa from their diameter distribution. Forest Ecology and Management, 313:55–62, 2014.
- 243 [18] S. W. Pacala, C. D. Canham, J. Saponara, J. A. Silander Jr., R. K. Kobe, and E. Ribbens. Forest models defined by field measurements: estimation, error analysis and dynamics. Ecological Monographs, 66(1):1–43, 1996.
- 246 [19] S. W. Pacala, C. D. Canham, and J. A. Silander Jr. Forest models defined by field measurements: I. the design of a northeastern forest simulator. Canadian Journal of Forest Research, 23:1980–1988, 1993.
- 249 [20] S. W. Pacala, C. D. Canham, J. A. Silander Jr., and R. K. Kobe. Sapling growth as a function of resources in a north temperate forest. Canadian Journal of Forest Research, 24:2172–2183, 1994.
- 252 [21] A. Porté and H. H. Bartelink. Modelling mixed forest growth: a review of models for forest management. Ecological Modelling, 150:141–188, 2002.

- 255 [22] E. Ribbens, J. A. Silander Jr., and S. W. Pacala. Seedling recruitment in forests: calibrating models to predict patterns of tree seedling dispersion. Ecology, 75(6):1794–1806, 1994.
- [23] W. E. Ricker. Stock and recruitment. Journal of the Fisheries Research Board of Canada, 11(5):559–623, 1954.
- 258
- [24] W. E. Ricker. Computation and interpretation of biological studies of fish populations. In Bulletin of the Fisheries Research Board of Canada, volume 191. Fisheries and Marine Service, Ottawa, 1975.
- 261
- [25] H. H. Shugart and D. C. West. Development of an appalachian deciduous forest succession model and its application to assessment of the impact of the chestnut blight. Journal of Environmental Management, 5:161–179, 1977.
- 264
- [26] H. L. Smith. Reduction of structured population models to threshold-type delay equations and functional differential equations: a case study. Mathematical Biosciences, 113:1–23, 1993.
- [27] H. L. Smith. A structured population model and a related functional differential equation: global attractors and uniform persistence. Journal of Dynamics and Differential Equations, 6(1):71–99, 1994.
- 267
- [28] N. Strigul, D. Pristinski, D. Purves, J. Dushoff, and S. Pacala. Scaling from trees to forests: tractable macroscopic equations for forest dynamics. Ecological Monographs, 78(4):523–545, 2008.
- 270
- [29] R. M. Teck and D. E. Hilt. Individual-tree diameter growth model for the northeastern united states. Research paper NE-649, US. Department of Agriculture, Forest Service, Northeastern Forest Experiment Station, Radnor, PA, 1991.
- 273
- [30] P. Trichet, D. Loustau, C. Lambrot, and S. Linder. Manipulating nutrient and water availability in a maritime pine plantation: effects on growth, production, and biomass allocation at canopy closure. Annals of Forest Science, 65(8):814, 2008.
- 276

- 279 [31] F. Valladares and Ü. Niinemets. Shade tolerance, a key plant feature of complex nature and consequences. Annual Review of Ecology, Evolution, and Systematics, 39:237–257, 2008.
- [32] M. A. Zavala, Ó. Angulo, R. B. de la Parra, and J. C. López-Marcos. An analytical model  
282 of stand dynamics as a function of tree growth, mortality and recruitment: The shade tolerance-stand structure hypothesis revisited. Journal of Theoretical Biology, 244:440–450, 2007.

Parameter	Interpretation	value	Reference
$\mu_{J_1}$	natural mortality rate for juveniles	0.03	estimated
$\mu_{A_1}$	natural mortality rate for adults	0.001	estimated
$\beta_1$	birth rate in absence of birth limitation	2	estimated
$s_-$	minimal size for juvenile	0	[19]
$s^*$	minimal size for adult	$\ln 50$	[22]
$\zeta_1$	parameter in the Ricker type function	0	estimated
$\tau_{01}$	time delay of the juveniles present at time 0 to become adults	121	estimated
$\alpha_1$	growth rate of juveniles without adults	0.1709	computed
$\delta_1$	parameter describing the descending speed of the growth rate when adult population increases	0.1	estimated

Table 1: Parameter values of the best fit for species 1: American beech.

Parameter	Interpretation	value	Reference
$\mu_{J_2}$	natural mortality rate for juveniles	0.031	estimated
$\mu_{A_2}$	natural mortality rate for adults	0.0037	estimated
$\beta_2$	birth rate in absence of birth limitation	4	estimated
$s_-$	minimal size for juvenile	0	[19]
$s^*$	minimal size for adult	ln 50	[22]
$\zeta_2$	parameter in the Ricker type function	0	estimated
$\tau_{02}$	time delay of the juveniles present at time 0 to become adults	127	estimated
$\alpha_2$	growth rate of juveniles without adults	0.249	computed
$\delta_2$	parameter describing the descending speed of the growth rate when adult population increases	0.1	estimated

Table 2: Parameter values of the best fit for species 2: eastern hemlock.

Parameter	Interpretation	value	Reference
$\zeta_{11}$	parameter in the competition term describing the intraspecific competition among American beech	1	estimated
$\zeta_{12}$	parameter in the competition term describing the interspecific influence of eastern hemlock on American beech	0.6	estimated
$\zeta_{21}$	parameter in the competition term describing the interspecific influence of American beech on eastern hemlock	1.6	estimated
$\zeta_{22}$	parameter in the competition term describing the intraspecific competition among eastern hemlock	1	estimated
$\tau_{01}$	time delay of the American beech juveniles present at time 0 to become adults	201	estimated
$\tau_{02}$	time delay of the eastern hemlock juveniles present at time 0 to become adults	208	estimated

Table 3: Other parameter values for two-species model.